Quantum stabilization of microcavity excitation in a coupled microcavity–half-cavity system

C. Y. Chang [1,*] Loïc Lanco,[2,3] and D. S. Citrin[4]

[1] *Georgia Institute of Technology, School of Physics, Atlanta, Georgia 30332-0250, USA*
[2] *Centre de Nanosciences et de Nanotechnologies, CNRS, Université Paris-Sud, Université Paris-Saclay, C2N, 91460 Marcoussis, France*
[3] *Université de Paris, F-75013 Paris, France*
[4] *School of Electrical and Computer Engineering, Georgia Institute of Technology, Atlanta, Georgia 30332-0250, USA and Georgia Tech - CNRS IRL-2958, Georgia Tech Lorraine, 2 Rue Marconi, 57070 Metz, France*

(Received 23 February 2019; revised manuscript received 14 December 2019; published 23 January 2020)

We analyze the quantum dynamics of a two-level emitter in a resonant microcavity with optical feedback provided by a distant mirror (i.e., a half cavity) with a focus on stabilizing the emitter-microcavity subsystem. Our treatment is fully carried out in the framework of cavity quantum electrodynamics. Specifically, we focus on the dynamics of a perturbed subradiant state of the emitter-microcavity subsystem to ascertain its stability (existence of time oscillatory solutions around the candidate state) or lack thereof. In particular, we find conditions under which multiple feedback modes of the half cavity contribute to the stability, showing certain analogies with the Lang-Kobayashi equations, which describe a laser diode subject to classical optical feedback.

DOI: 10.1103/PhysRevB.101.024305

I. INTRODUCTION

With recent advances in the fabrication of nanophotonic structures, there is an increasing ability to control and manipulate the optical properties on the single-photon level [1–3]. One of the techniques central to such control is the ability to access the strong-coupling regime of cavity quantum electrodynamics (cQED). In solid-state structures, recent developments include coupling quantum emitters such as quantum dots to photonic crystals [4–6] and micropillar cavities [7,8]. These devices provide unidirectional photons that are of interest, for example, to improve quantum communications over long distances [9]. In addition, the ability to control and coherently manipulate photons coupled to the internal state of the quantum dot is of great importance due to potential applications in quantum memory and quantum information processing [10].

Controlling a quantum system—in the sense of providing stabilization of its quantum state—presents a nontrivial problem. The use of feedback to provide stabilization in classical systems is quite advanced, while less is known for quantum systems. Two feedback-control schemes have been explored recently in quantum optics, *viz.*, measurement-based and coherent feedback loops [11,12]. In a measurement-based feedback loop, the quantum system is monitored and the outcome of the measurement is used as *classical* information to manipulate the operations. A measurement-based feedback loop has been implemented in a cQED system with trapped atoms [13]. In coherent feedback, the dynamics are entirely quantum mechanical and the system interacts coherently with an ancillary subsystem in both the extraction and manipulation processes. For coherent feedback, such as Pyragas feedback [14], both processes utilize information stored in the reservoir degrees of freedom residing, for example, in an external cavity.

Canonical consideration

Before embarking on our study, it is necessary to discuss some of the various aspects of our analysis that are likely to be unfamiliar to many readers. Given that the measurement process will unavoidably collapse the wave function, measurement-based feedback presents limitations when the target state is a superposition. To implement coherent quantum feedback in quantum optics, one typical configuration consists in coupling the quantum system with an external half cavity, having a perfect mirror at the opposite end, as illustrated in Fig. 1(a). Here, we introduce a quantum dot coupled to a microcavity as our quantum system, similar to the time-delayed feedback setup used in an external-cavity laser.

The presence of time-delayed feedback is known for the external-cavity laser to generate multiple steady-state solutions. The stable modes of the external cavity are called external cavity modes, while the unstable modes of the external cavity are known as antimodes [15]. Depending on the various parameters of the system (e.g., injection current, feedback strength, and external cavity length L), various dynamics can occur near and amongst these solutions [16,17]. In particular, oscillatory dynamics about various external cavity modes occur in certain parameter regimes, and are closely related to undamped relaxation oscillations [18], while more complex behavior exhibiting closed trajectories encircling one or more steady-state solutions are also observed. The emergence of multiple solutions is often seen in many nonlinear systems, but not in a quantum system with a finite number of degrees of freedom [19]. However, in quantum systems with a bath

*Present address: Quantum Functional System Research Group, Center for Emergent Matter Science, RIKEN, Wakoshi, Japan; chien-yuan.chang@riken.jp

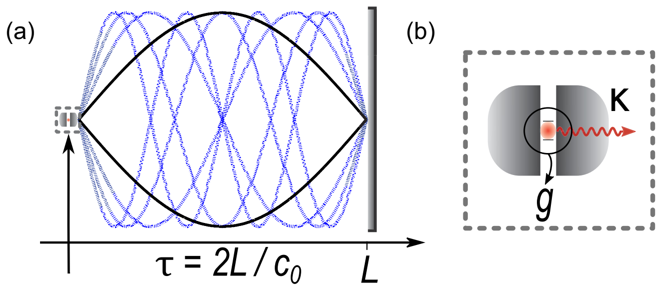

FIG. 1. (a) The quantum dot–microcavity system coupled to an external cavity of length L in which a quasicontinuum of photon modes exist. τ is the delay time of the coherent feedback. The black and blue curves indicate classical electric fields forming standing waves from the external cavity. (b) Schematic of a two-level quantum dot in a near-resonant microcavity, where g is the coupling strength and $\kappa = \pi G_0^2/(2c_0)$ is the microcavity damping rate.

of infinite degrees of freedom (in our case, the modes of the external cavity), once these are integrated out, the system may exhibit what appears to be nonlinear behavior in the remaining explicitly considered degrees of freedom.

Broadly speaking, two approaches have been used to account for the coherent feedback. In one approach, the non-Markovian evolution of the coherent feedback effect is analyzed with a differential equation with a time propagator [20]. On the other hand, the optical feedback from a mirror has typically been accounted for using a one-dimensional model for the electromagnetic field with a standing-wave basis in the Markovian limit [21–23]. Recent theoretical studies have focused on Markovian coherent feedback [21–32]. It has been demonstrated that the standing-wave field model in a half cavity (Markovian) is equivalent to a time-delayed feedback system (non-Markovian) [23,31]. The control of the delay time can be a key factor in the stability or instability as well as the nonlinear dynamics in many complex systems [33,34], providing wide-range applications. These works provide a promising route to rapid convergence of states [34], enhancing entangled photon-pair generation from biexcitons [35], and to drive continuous exchanges for pure states [30]. Among these studies, stability in coherent feedback systems has been investigated by Grimsmo [20] based on linear delayed differential equations (non-Markovian). Since then, few other studies have focused on stability and its relation to time-delayed systems [36,37]. The evolution of the quantum states in these investigations is described by means of a time-varying Hamiltonian. These works are focused on specific features of the quantum system and not on the stability of the target state, which from the standpoint of experimental realization or practical application is of key importance.

In this study, we consider a quantum system composed of a single-photon emitter in the form of a quantum dot within a microcavity formed by a micropillar with coherent quantum feedback provided by a distant mirror as shown in Fig. 1(a). Our approach presents a direct stability analysis in the Markovian dynamics of quantum feedback from a single-photon emitter. The quantum feedback is achieved via the external cavity, similar to previous studies [30,31].

Since photon leakage from the external cavity is neglected, our system conserves the excitation number. Our focus is on the one-excitation subspace. In the one-excitation subspace, we find the steady-state solutions, which we then investigate for stability. By *steady* state, we mean states in which the amplitude coefficients remain constant in magnitude (i.e., stationary population), and evolve in phase with constant angular frequencies. Therefore, steady states are those that are simultaneously eigenstates of both the noninteracting and the interacting Hamiltonians. We explore the stability of the steady states, that is, states of the composite microcavity/quantum dot subsystem that are effectively decoupled from the external cavity. We find that the *stable* steady states are represented by the microcavity/quantum dot and its mirrored self being in an antisymmetric singlet state [38]. Similar observations have been made that the singlet state corresponds to the Dicke subradiant state [39] in a waveguide system [24], in a system with chiral feedback from a single V-level atom [40]. To be more specific, the singlet state would appear effectively decoupled from the external cavity, being in a stable subradiant state, whereas the symmetric state is superradiant, and thus unstable, as it decays at twice the cavity damping rate from the microcavity [24,40]. In the case with one single-photon emitter coupled to the external cavity, the subradiant state would be the only steady state where the population in quantum dot and microcavity are antisymmetric [39].

We determine the stability by studying the dynamics in the vicinity of the steady state. This is done by constructing the Jacobian matrix of the linearized equations of motion with the state amplitudes perturbed from the steady state [19], a technique widely employed for classical stability analysis. We analyze the eigenvalues of the Jacobian matrix as a function of coupling strength between the microcavity and external cavity. A strictly imaginary eigenvalue indicates oscillatory dynamics about the candidate steady state, which is thus deemed stable while a positive (negative) *real part* of the complex eigenvalues indicates unstable (stable) steady states. The effects of time delay are also studied for various external cavity length L. We numerically verify the Jacobian analysis by perturbing the steady state to investigate its stability, which agrees with the results obtained directly from the Jacobian of the state amplitudes.

The remainder of the paper is organized as follows. In the next section, we outline the cQED description of the system. We next find the steady state. Following this, we assess the steady state's stability. In the final section, we conclude.

II. THEORETICAL DESCRIPTION OF THE SINGLE-EMITTER, MICROCAVITY, EXTERNAL CAVITY SYSTEM

We begin by introducing the system. We consider an intrinsic quantum dot coupled to a single near-resonant mode of a high-Q micropillar microcavity [Fig. 1(b)] and coupled in turn to the external cavity modes shown in Fig. 1(a). The quantum dot is characterized by interband-transition frequency ω_0. The quantum dot interband transition is dipole coupled to a single mode of the micropillar microcavity of angular frequency ω_{MC} (in this study, we will eventually take $\omega_{\mathrm{MC}} = \omega_0$) with coupling strength g, as in Ref. [41]. This approach can yield strong coupling between the quantum dot and the microcavity [35] and can generate high-purity, indistinguishable single photons [41]. We place an ideal mirror with reflection coefficient $r = -1$ a distance $L = c_0\tau/2$ from the micropillar to form the external cavity (half cavity), with c_0 the speed of light in vacuum and τ the external cavity round-trip feedback time. The conditions we choose are similar to the single quantum dot in a microcavity subjected to an external mirror in a recent paper [31]. For a mirror with $|r| < 1$, the coherent feedback can be treated considering the mirror properties [42], while analysis can be performed using an open quantum-system formalism, discussed in a recent publication by Whalem [43].

We work in the rotating-wave approximation (RWA) [44] in the Schrödinger picture as in Refs. [21,30,31]. The derivation of the interaction Hamiltonian can be found in Refs. [21,30–32,44–46] (see the Supplemental Material [47]). For the external cavity, we use the free-space dispersion for photons, $\omega_k = c_0|k|$, assuming a sufficiently large value of L so that the photon modes can be considered a quasicontinuum. We assume that only the optical modes with angular frequencies near ω_0 interact strongly with the microcavity photon ($\omega_k \approx \omega_{\rm MC} \approx \omega_0$). We obtain the following interaction Hamiltonian describing the quantum dot coupled to the microcavity mode and that mode in turn coupled to the external cavity modes:

$$\frac{H_{\rm int}^{\rm (RWA)}}{\hbar} = -\omega_g(\sigma^- a^\dagger + \sigma^+ a) - \int_{-\infty}^{\infty} d\omega_k [G(k,t) a^\dagger b_k + \text{H.c.}], \qquad (1)$$

with $\omega_g = g/\hbar$, $a^\dagger$ (a) the creation (annihilation) operator for the microcavity photon, and $\sigma^{+(-)}$ the raising (lowering) operator of the two-level quantum dot system. The bosonic operators b_k destroy a photon of frequency ω_k in the external cavity as defined as in Ref. [32] and the coupling element, $G(k,t) = G_0 \sin(kL) e^{i(\omega_0-\omega_k)t}$, where $G_0 = \sqrt{2c_0\kappa/\pi}$. Note that because $H_{\rm int}^{\rm (RWA)}$ is quadratic in creation and annihilation operators, the Hamiltonian conserves the number of excitations. We extend the lower limit of integration to $-\infty$ given the interaction bandwidth is narrow compared with ω_0. A detailed discussion is presented in the Supplemental Material [47].

We now concentrate on the one-excitation subspace where an arbitrary wave function can be written

$$\Psi(t) = c_e(t)\,|e,0,0\rangle + c_c(t)\,|g,1,0\rangle + \int_{-\infty}^{\infty} c_k(t)\,|g,0,k\rangle\, dk. \qquad (2)$$

Here, in kets $|a,b,k\rangle$, $a = e$ (g) denotes the quantum dot in the excited (ground) state; $b = 0$ (1) denotes zero (one) microcavity photon; and k denotes the external cavity photon wave vector. $\Psi(t)$ is thus described by the time-dependent amplitudes $c_e(t)$, $c_c(t)$, and $c_k(t)$.

III. STEADY STATE

Substituting $\Psi(t)$ into the time-dependent Schrödinger's equation, we obtain the following coupled equations of motion (EOMs) for the time-dependent amplitudes:

$$\frac{\partial c_e}{\partial t} = i\omega_g\, c_c, \qquad (3)$$

$$\frac{\partial c_c}{\partial t} = i\omega_g\, c_e + i\int_{-\infty}^{\infty} c_k\, G(k,t)\, dk, \qquad (4)$$

$$\frac{\partial c_k}{\partial t} = iG^*(k,t)\, c_c. \qquad (5)$$

To find the steady states (*steady* in the more narrow sense defined above), we write $c_i(t) = |c_i(t)| \exp[i\theta_i(t)]$, to obtain a new set of EOMs,

$$\frac{\partial c_i}{\partial t} = \frac{\partial |c_i|}{\partial t} e^{i\theta_i(t)} + i\frac{\partial \theta_i(t)}{\partial t} |c_i| e^{i\theta_i(t)}, \qquad (6)$$

with $i = e$, c, and k. We apply the constraint for a steady state ($|c_i|$ and $\dot{\theta}_i$ all constants) and find the solution as discussed in the Supplemental Material [47].

We denote the steady state (with respect to the interaction Hamiltonian) in the single-excitation subspace as $\bar{\Psi}(t)$ (where the bar indicates a steady-state solution). In the frame rotating at ω_0, $\bar{\Psi}_{\rm RWA}(t) = \bar{\Psi}(t) e^{-i\omega_0 t}$,

$$\bar{\Psi}_{\rm RWA}(t) = \bar{c}_e(t)\,|e,0,0\rangle + \bar{c}_c(t)\,|g,1,0\rangle + \int_{-\infty}^{\infty} \bar{c}_k(t)\,|g,0,k\rangle\, dk.$$

We thus obtain the noninteracting amplitudes for the steady state,

$$\bar{c}_e(t) = -\alpha e^{-i\omega_g t}, \qquad (7)$$

$$\bar{c}_c(t) = \alpha e^{-i\omega_g t}, \qquad (8)$$

$$\bar{c}_k(k,t) = \frac{\alpha G_0 \sin(kL)}{\omega_k - \omega_g - \omega_0} e^{i(\omega_k-\omega_g-\omega_0)t}. \qquad (9)$$

Note that the strict commensurability condition, i.e., $2L/c_0 = n2\pi/(\omega_0 + \omega_g)$ with $n \in \mathbb{N}$, is required for the steady state. Detailed reasons will be explained later in this work and can also be found in Refs. [25,31]. The parameter α is defined in the next paragraph. Note that the minus sign results from the microcavity/quantum dot being in a singlet state (antisymmetric) of the quantum system and its mirrored self [23,24,38,40]. In this state, the quantum dot–microcavity subsystem is effectively decoupled from the external cavity, thus being in a subradiant state, as discussed for similar systems in Refs. [24,38,40].

The noninteracting amplitudes associated with this steady state can be characterized by a single parameter,

$$\alpha = |c_c(t)| = |c_e(t)| = \left(2 + \frac{\pi G_0^2 L}{c_0^2}\right)^{-1/2} = (2 + \tau\kappa)^{-1/2},$$

where recall $G_0 = \sqrt{2c_0\kappa/\pi}$ and κ is the microcavity photon damping rate. Since we consider 100% reflection from the distant mirror ($r = -1$ in this study), the damping rate characterizes both the rate *into the external cavity* and *the feedback rate from the reflected photon.*

The steady state is indicated in the frame rotating at ω_0 in Fig. 2. The blue arrow shows the state of the quantum dot at a snapshot in time, with the time evolution in the RWA shown by the orange arrows, where we

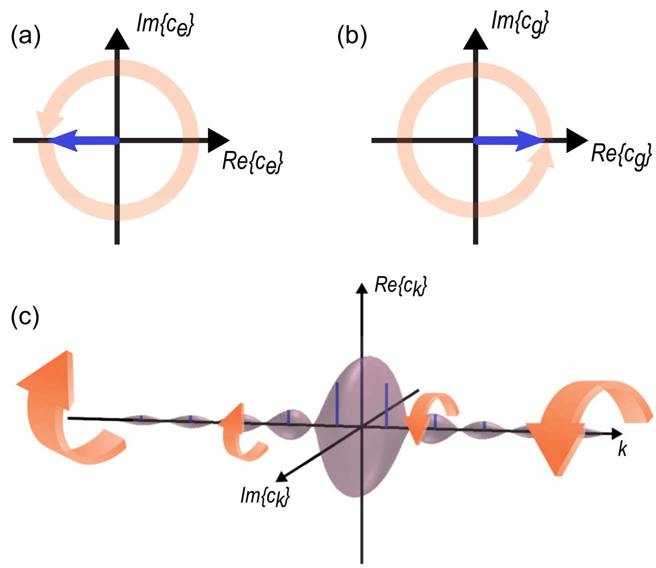

FIG. 2. Representation of the one-excitation steady state in the frame rotating at the frequency ω_0 (a) $\bar{c}_e(t)$, (b) $\bar{c}_c(t)$, and (c) $\bar{c}_k(k,t)$. The blue arrows indicate the initial condition and the orange arrows indicates the time evolution.

choose initial conditions $\bar{c}_e(0)=\alpha$, $\bar{c}_c(0)=-\alpha$, and $\bar{c}_k(k,0)=\alpha G_0 \sin(kL)/(\omega_k-\omega_0-\omega_g)$. In this case, the external cavity photon is in a standing wave and its population is described by a sinc function in the k channel (of frequency ω_k), centered on $\omega_k=\omega_0+\omega_g$, i.e., $kL=n\pi$, with n an integer number such that the commensurability condition is fulfilled: $(\omega_0+\omega_g)\tau=2n\pi$. Note that each external cavity state c_k revolves around the k axis at different rate, as illustrated in Fig. 2(c).

The evolution of the microcavity photon population $|c_c(t)|^2$ is plotted in Fig. 3. The theoretical and numerical results for the steady state just found are plotted in the black and yellow dotted curves, respectively. In this case, the microcavity photon population remains constant in time. The green curve (case II) plots the microcavity photon population $|c_c|^2$, however, for the initial state $c_e(0)=1$, $c_c(0)=0$, $c_k(0)=0$ for

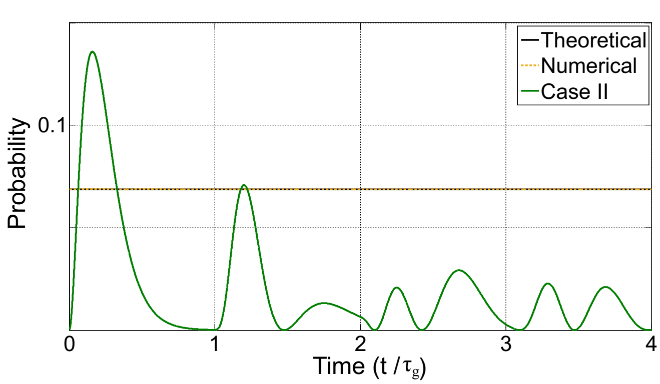

FIG. 3. Time evolution of the probabilities of $|c_c(t)|^2$ for various initial conditions. The quantum dot is initialized in the excited state for the green curve (case II); however, choosing initial conditions corresponding to a steady state results in $|c_c(t)|^2$ being independent of time (black and dotted yellow curves).

all k. In this case, the microcavity photon population varies significantly at first and eventually mainly leaks out into the external cavity. Note that there is only one steady state in our sense within the one-excitation subspace.

To lend insight into the nature of the steady state, the initial state amplitudes of the external cavity photons of wave number $\bar{c}_k(k,0)$ are an *even* function, centered on $\omega_k=\omega_g+\omega_0$, i.e., $kL=n\pi$ while the coupling $G(k,t)$ is an *odd* function centered on $\omega_k=\omega_g+\omega_0$. Thus, while L satisfies the commensurability condition, the external cavity is in effect decoupled from the microcavity photon and the quantum dot for the steady state. As this occurs, the quantum dot and the microcavity photon experience a cavity-assisted interaction at the rate of ω_g, and both quantum dot and microcavity photon state are stable state, when their complex amplitudes are π out of phase. The only steady state corresponding to the interaction Hamiltonian is antisymmetric in the amplitudes c_e and c_c, and similar to the bound state in Refs. [25,28,29] or the subradiant state in the recent studies of Refs. [40,48].

IV. STABILITY ANALYSIS

In the previous section we identified a steady state in the one-excitation subspace. In this section, we ascertain the steady state's stability, which depends on two important parameters. The first parameter is n, related to ω_g and to the external cavity round-trip time τ. The second one is the ratio $R=\kappa/4g$, between the cavity damping rate κ and the coupling strength g. The reflected photon is assumed to undergo a π phase change from an ideal mirror ($r=-1$ in this study). To begin, we constructed a Markovian model to numerically simulate the evolution based on Eqs. (3)–(5), and the stationarity of $\bar{\Psi}$ is demonstrated in Fig. 3. For example, for $c_e(0)=1$, $c_c(0)=0$, and $c_k(0)=0$ for all k, the microcavity photon population exhibits nonperiodic oscillations on the time scale of vacuum-field Rabi oscillations, shown in Ref. [35].

Next, we study the dynamics in the vicinity of the steady state to ascertain its stability. We expect that for a stable state, the probabilities will remain near the initial values. Here, we perturb the steady state and track the dynamics. (This numerical approach is infeasible *rigorously* to determine the stability of the candidate steady state due to the existence of numerous degrees of freedom that would have to be perturbed individually; indeed, this is, in effect, what the method below of computing the eigenvalues of the Jacobian does for us.) We add small values $\delta_{c,i}$ to the initial conditions for c_e and c_c with respect to the steady state $\bar{\Psi}(t)$ in Eqs. (6)–(8), *viz.*, $\delta c_c=[\pm 0.01, \pm 0.02]\alpha$ while the amplitude of the quantum dot state $c_e(0)$ is perturbed such that $|\bar{c}_e+\delta c_e|^2+|\bar{c}_c+\delta c_c|^2=|\bar{c}_e|^2+|\bar{c}_c|^2$. We shall see that the nature of the stable state depends crucially on the ratio $R=\kappa/(4g)$ between the microcavity damping rate κ and the coupling strength g, the inversion of the conventional coupling strength parameter between a two-level system and a cavity, where $R<1$ ($R>1$) indicates the strong- (weak-)coupling regime [49]. Small R thus means the vacuum-field Rabi frequency is much larger than the microcavity photon leakage rate; large R indicates a relatively high microcavity photon leakage rate compared with the vacuum-field Rabi frequency. The effect on the

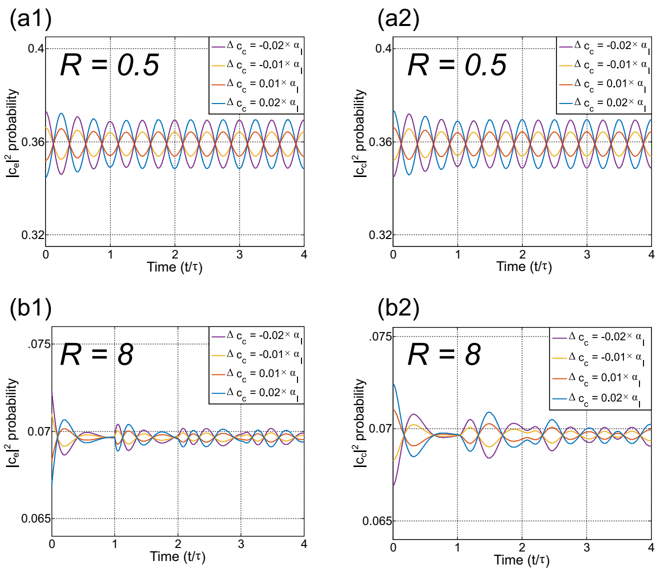

FIG. 4. The evolution $|c_e(t)|^2$ and $|c_c(t)|^2$ of perturbed steady states with various values of R. Note that the various probabilities remain near the initial values, indicating likely stability.

stability is illustrated by plotting the probability for $R = 0.5$ and $R = 8$. The probabilities of the excited quantum dot state, $|c_e(t)|^2$, are plotted in Figs. 4(a1) and 4(b1) and microcavity photon state $|c_c(t)|^2$ in Figs. 4(a2) and 4(b2) for $R = 0.5$ and 8, respectively. We note that $n = 1$ in Fig. 3 and all cases in Fig. 4

In Figs. 4(a1) and 4(a2), for small R (strong coupling), the variation of the probability from its mean value exhibits oscillations at roughly the vacuum-field Rabi frequency $2\omega_g$ with some initial damping from $t = 0$ to τ at rate 2κ. For $t \gtrsim \tau$, the damping is arrested and oscillations at the vacuum-field Rabi frequency persist. By comparison, for $R = 8$ [Figs. 4(b1) and 4(b2)] when vacuum-field Rabi oscillations do not have a chance to occur before photon leakage from the microcavity, the dynamics of both probabilities are not evidently periodic, indicating the participation of multiple frequencies. We shall see this is due to the participation of many coupled external-cavity-like modes.

In order to explore the stability of the steady state in a rigorous fashion, we consider an analysis of the eigenvalues of the Jacobian matrix [50] to confirm the foregoing numerical simulations. The Jacobian is defined as the matrix of all first-order partial derivatives with respect to the each variable (in this case, the perturbed state amplitudes) evaluated for the steady state [19]. In other words, the Jacobian probes the change in the steady state with respect to an arbitrary infinitesimal perturbation. Its eigenvalues, therefore, indicate whether or not the state is stable, with a tendency to oscillate around the steady state for eigenvalues being strictly *imaginary*, to be stable and evolve toward a steady state for *real parts* of all eigenvalues being negative, or to be unstable and to evolve away from the steady state (all *real parts* of any complex eigenvalues being positive). In addition, saddle points are also possible where the steady state is stable against perturbations in certain directions in state space, but not in others.

More specifically, the Jacobian matrix $\boldsymbol{J_\delta}$ (see the Supplemental Material for definition [47]) satisfies the equation

$$\frac{\partial}{\partial t}\delta c_i(t) = \boldsymbol{J_\delta}\delta c_i(t). \tag{10}$$

We begin by studying the Jacobian matrix constructed with linearized EOMs of the perturbed state. The perturbed states along the i direction in state space from the steady state will evolve according to $\delta c_i(t) = \delta c_i(0)e^{\lambda_i t}$ where λ_i is the eigenvalue along the i direction and $\delta c_i(t)$ is the small perturbation along the i vector from the steady state $\bar{c}_\alpha$ at $t = 0$. Given the eigenvalues, possible cases for the steady state are attractors, repellers, or saddle points corresponding to all negative, all positive, or some positive and some negative eigenvalues, respectively. The dynamics can be analyzed by the nature of the equilibrium state, in this case, the steady state, $\bar{\Psi}(t)$ in Eqs. (7)–(9).

The interaction of the perturbed state amplitudes can be derived using linearized EOMs near the steady state, and the Jacobian matrix of rank $(2 + N)$ is derived following the small-signal model, where N is the number of external cavity photon states c_k used in the simulation. Note that Jacobian, $\boldsymbol{J_\delta}$, is derived from linearization at the steady state and is found to be a rank-$N + 2$ skew Hermitian matrix, while the interaction Hamiltonian is a rank-2 Hermitian matrix in the one-excitation subspace.

We proceed to analyze the stability of the steady state by considering the eigenvalues, λ_is, of $\boldsymbol{J_\delta}$. We focus on the dependence of the eigenvalues on the ratio $R = 4\kappa/g$ between the microcavity photon damping rate and the quantum dot–microcavity coupling strength. By solving the characteristic equation of $\boldsymbol{J_\delta}$, we find all the eigenvalues are purely imaginary ($i\lambda_i \in \mathbb{R}$). These imaginary eigenvalues indicate oscillatory dynamics upon perturbation about the steady state, i.e., this indicates stability. Notably, since the perturbation of the steady state evolves following $\delta c_c(t) = \delta c_c(0)\exp(\lambda_c t)$, we expect to observe oscillation in the probabilities both for the quantum dot excited state and for the microcavity photon $|c_c(t)|^2 = \alpha^2 + 2\alpha\delta c_c(0)\cos\omega_{\rm osc}t + |\delta c_c(0)|^2$, where $\omega_{\rm osc}(\lambda) = \omega_0 + \omega_g - i\lambda_c$. The eigenvalues of the Jacobian are solutions of the determinental equation $|\boldsymbol{J_\delta} - \lambda \mathrm{I}_{(2+\mathrm{N_k})}| = 0$. One finds

$$(\omega_{\rm osc} - \omega_g)^2 - \kappa(\omega_{\rm osc} - \omega_g)\sin(\omega_{\rm osc}\tau) - \omega_g^2 = 0. \tag{11}$$

Here, we focus on finding the frequency $\omega_{\rm osc}(\lambda_c)$ as a function of the parameter $R = \kappa/(4g)$ of different time delay τ. Given the wide range of R investigated, the following results are plotted using a horizontal scale in $\log_2 R$. The detailed derivation is presented in the Supplemental Material [47]. In addition, we carry out this analysis focusing on adjusting the parameters, external cavity round-trip time τ. We consider the effect of varying τ, restricting its value to integer multiples of $\tau_g = 2\pi/\omega_g$. We explore the stability dependence on R for various time delay. Particularly, in Fig. 5, we explore the cases where the time delay, $\tau = n\,\tau_g$, is an integer multiple of τ_g where $\tau_g = 2\pi/\omega_g$, and $n \in \mathbb{N}$.

In the case of coherent quantum feedback from a single photon, one can show that the *product* of the time delay τ and the dimensionless ratio $\bar{R}(n)$ is constant $1/(2\pi)$ for $n \in \mathbb{N}$ from Eq. (11). We find the critical value $\bar{R}$ of R,

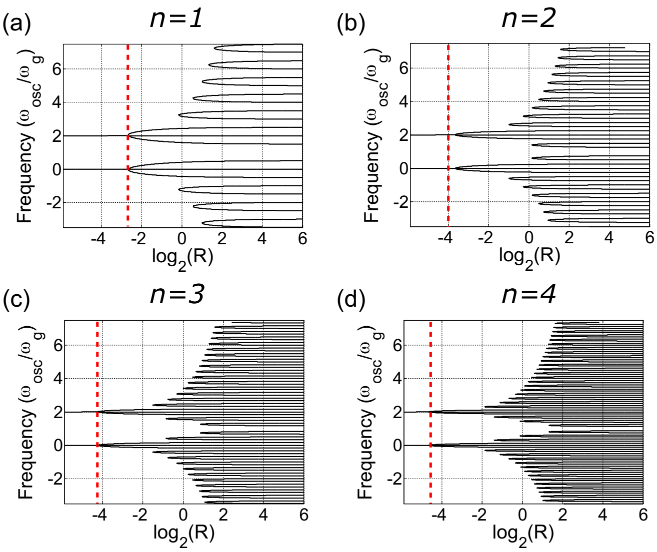

FIG. 5. Frequencies of oscillation $\omega_{\rm osc}$ about the steady state of the probability $|c_c(t)|^2$ as a function of $\log_2 R$ for various τ_g. The frequency is obtained from $\omega_{\rm osc} = \omega_g + \omega_0 - i\lambda$.

beyond which more than two (imaginary) eigenvalues of the Jacobian matrix appear decreases as L increases shown by various vertical dotted red lines in the panels of Fig. 5. That is, $\bar{R}(1) = 0.16$ [$\log_2 \bar{R}(1) = -2.74$], $\bar{R}(2) = 0.08$ [$\log_2 \bar{R}(2) = -3.64$], $\bar{R}(3) = 0.053$ [$\log_2 \bar{R}(3) = -4.24$], and $\bar{R}(4) = 0.039$ [$\log_2 \bar{R}(4) = -4.68$].

The dynamics of external-cavity lasers have been intensively studied based on the semiclassical Lang-Kobayashi equations [51,52]. The Lang-Kobayashi equations describe the nonlinear dynamics of the electric-field amplitude $|E|$, carrier density n in the active region, and optical phase $\Delta\phi$ by a set of equations of motions in the form of coupled delayed-differential equations. In the Lang-Kobayashi model for an external-cavity laser, this product is also proportional to the dimensionless parameter $C = \gamma\tau$ characterizing feedback strength defined in Ref. [53], where γ is the *feedback parameter*. Specifically, in the theoretical study of weak optical feedback (classical external-cavity laser), $C < 1$ there is always *one* stable solution; for $C > 1$ there may exist more stable solutions corresponding to single-frequency operation [53]. The frequency difference between the multiple solution of $\omega_{\rm osc}$ scales linearly with n as one would expect from the Lang-Kobayashi model. As we pointed out in the previous paragraph, the critical value $\bar{R}$ in the single-photon limit corresponds up to a constant multiplicative factor to the feedback parameter, γ in the classical regime. That is, $\bar{R}$ satisfies the relationship $n\bar{R} = 1/(2\pi)$ [$\tau\bar{R} = \tau_g/(2\pi)$], representing the feedback parameter in the single-photon regime.

V. DISCUSSION AND CONCLUSION

The implementation of coherence feedback with few-excitation states incorporating cQED systems can be realized in various ways. Albert *et al.* have realized coherent optical feedback with a microlaser, where chaotic behavior is observed with self-feedback for a few photons, ~100, and studied the second-order autocorrelation function $g^{(2)}(\tau)$ [54]. Note that, to describe the dynamics in these experiments, many realistic parameters have to be taken into account, including the quantum dot dephasing rate, the quantum dot decay rate, the transmission and reflection coefficients of the external cavity mirror, and the microcavity–external-cavity coupling. However, these parameters describe the loss channels and contribute to the decay of the probabilities. Comparing to the ideal scenario described in this paper, we expect that these parameters will weakly influence the oscillation frequencies provided the large R limit can be reached.

A stability analysis of the type implemented here can also be applied to the subradiant state existing in a quantum dimer system with a coupled cavity [40,48] or in certain spin systems [55,56]. In the case with a spin system, the coupling element between two interacting spins placed at a distance L apart is replaced by $G_{sd}(k', t) = G_0 \cos(k'L)e^{i(\omega_0-\omega_k)t}$ [55]. By making the transformation $k' = k - \pi/2$, we obtain the relationship between the eigenvalues in two cases, i.e., the eigenvalues of $\lambda_{sd} = \lambda - \pi/2$. Following the derivation of this work, we can solve the emergent behavior of the additional solutions of $\omega_{{\rm osc},sd}(R, n) = \omega_{\rm osc}(R, n)$ near the steady state. Thus, the dynamical behaviors of the interacting quantum dimer coupled through a (single) photon bath should behave similarly to coherent quantum feedback. In this case, the frequencies appearing in Figs. 5(a) and 5(b) must be interchanged as well as those appearing in Figs. 5(c) and 5(d).

In conclusion, we consider a system composed of a quantum dot in a microcavity coupled to an external cavity and find a steady state where the state initialized in the microcavity and quantum dot degrees of freedom is stable against decay into external cavity photons. Specifically, we give the analytical expression for the steady solution for such a system in the one-excitation subspace. We find that this state is stable by performing stability analysis on the Jacobian of state amplitudes. The periodic solutions perturbed about the steady state, obtained from the eigenvalues of the Jacobian, indicate that additional solutions arise above a critical value $\bar{R}$ or R as experimental parameters such as the cavity damping rate, the cavity coupling strength, and the external cavity length are varied. We found a strong similarity to the Lang-Kobayashi model in this behavior in terms of its dependence on τ. In addition, numerical simulation verifies these results, showing that interesting dynamics appear in the vicinity of the steady states. Our stability analysis may serve as a bridge between classical and quantum models for nanophotonic structures subject to optical feedback.

ACKNOWLEDGMENTS

We appreciate the kind and fruitful discussion with Prof. P. Senellart. In addition, we thank Dr. Y.-L. L. Fang for useful discussions. The authors gratefully acknowledge the financial support of the 2015 Technologies Incubation scholarship for Dr. C. Y. Chang from the Ministry of Education, Taiwan.

[1] J. McKeever, A. Boca, A. D. Boozer, J. R. Buck, and H. J. Kimble, Nature (London) **425**, 268 (1997).
[2] P. Lodahl, S. Mahmoodian, and S. Stobbe, Rev. Mod. Phys. **87**, 347 (2015).
[3] A. Reiserer and G. Rempe, Rev. Mod. Phys. **87**, 1379 (2015).
[4] P. Lodahl, A. F. Van Driel, I. S. Nikolaev, A. Irman *et al.*, Nature (London) **430**, 654 (2004).
[5] I. Söllner, S. Mahmoodian, S. L. Hansen, L. Midolo, A. Javadi, G. Kiršanskė, T. Pregnolato, H. El-Ella, E. H. Lee, J. D. Song *et al.*, Nat. Nanotechnol. **10**, 775 (2015).
[6] M. Nomura, N. Kumagai, S. Iwamoto, Y. Ota, and Y. Arakawa, Nat. Phys. **6**, 279 (2010).
[7] C. Böckler, S. Reitzenstein, C. Kistner, R. Debusmann, A. Löffler, T. Kida, S. Höfling, A. Forchel, L. Grenouillet, J. Claudon *et al.*, Appl. Phys. Lett. **92**, 091107 (2008).
[8] O. Gazzano, S. M. de Vasconcellos, C. Arnold, A. Nowak, E. Galopin, I. Sagnes, L. Lanco, A. Lemaître, and P. Senellart, Nat. Commun. **4**, 1425 (2013).
[9] D. Bouwmeester, J.-W. Pan, K. Mattle, M. Eibl, H. Weinfurter, and A. Zeilinger, Nature (London) **390**, 575 (1997).
[10] V. Giesz, N. Somaschi, G. Hornecker, T. Grange, B. Reznychenko, L. De Santis, J. Demory, C. Gomez, I. Sagnes, A. Lemaître *et al.*, Nat. Commun. **7**, 11986 (2016).
[11] A. Serafini, ISRN Optics **2012**, 275016 (2012).
[12] H. M. Wiseman and G. J. Milburn, *Quantum Measurement and Control* (Cambridge University Press, Cambridge, UK, 2009).
[13] H. M. Wiseman and G. J. Milburn, Phys. Rev. Lett. **70**, 548 (1993).
[14] K. Pyragas, Phys. Lett. A **170**, 421 (1992).
[15] C. Henry and R. Kazarinov, IEEE J. Quantum Electron. **22**, 294 (1986).
[16] M. Wolfrum and S. Yanchuk, Phys. Rev. Lett. **96**, 220201 (2006).
[17] K. Green, J. Comput. Appl. Math. **233**, 2405 (2010).
[18] T. Erneux, E. A. Viktorov, and P. Mandel, Phys. Rev. A **76**, 023819 (2007).
[19] W. Eckhaus, *Studies in Nonlinear Stability Theory*, Springer Tracts in Natural Philosophy Vol. 6 (Springer-Verlag, New York, 1965).
[20] A. L. Grimsmo, Phys. Rev. Lett. **115**, 060402 (2015).
[21] R. J. Cook and P. W. Milonni, Phys. Rev. A **35**, 5081 (1987).
[22] U. Dorner and P. Zoller, Phys. Rev. A **66**, 023816 (2002).
[23] A. Beige, J. Pachos, and H. Walther, Phys. Rev. A **66**, 063801 (2002).
[24] D. E. Chang, L. Jiang, A. Gorshkov, and H. Kimble, New J. Phys. **14**, 063003 (2012).
[25] Yao-Lung L. Fang, H. U. Baranger, Phys. Rev. A **91**, 053845 (2015).
[26] P.-O. Guimond, M. Pletyukhov, H. Pichler, and P. Zoller, Quantum Sci. Technol. **2**, 044012 (2017).
[27] I.-C. Hoi, A. F. Kockum, L. Tornberg, A. Pourkabirian, G. Johansson, P. Delsing, and C. Wilson, Nat. Phys. **11**, 1045 (2015).
[28] T. Tufarelli, M. S. Kim, and F. Ciccarello, Phys. Rev. A **90**, 012113 (2014).
[29] G. Calajó, Y. Y. L. Fang, H. U. Baranger, and F. Ciccarello, Phys. Rev. Lett. **122**, 073601 (2019).
[30] A. Carmele, J. Kabuss, F. Schulze, S. Reitzenstein, and A. Knorr, Phys. Rev. Lett. **110**, 013601 (2013).
[31] J. Kabuss, D. O. Krimer, S. Rotter, K. Stannigel, A. Knorr, and A. Carmele, Phys. Rev. A **92**, 053801 (2015).
[32] H. Pichler and P. Zoller, Phys. Rev. Lett. **116**, 093601 (2016).
[33] M. C. Soriano, J. García-Ojalvo, C. R. Mirasso, and I. Fischer, Rev. Mod. Phys. **85**, 421 (2013).
[34] A. L. Grimsmo, A. Parkins, and B. Skagerstam, New J. Phys. **16**, 065004 (2014).
[35] S. M. Hein, F. Schulze, A. Carmele, and A. Knorr, Phys. Rev. Lett. **113**, 027401 (2014).
[36] N. Német and S. Parkins, Phys. Rev. A **94**, 023809 (2016).
[37] G. Tabak and H. Mabuchi, EPJ Quantum Technol. **3**, 3 (2016).
[38] P. A. Vetter, L. Wang, D.-W. Wang, and M. O. Scully, Phys. Scr. **91**, 023007 (2016).
[39] R. H. Dicke, Phys. Rev. **93**, 99 (1954).
[40] P.-O. Guimond, H. Pichler, A. Rauschenbeutel, and P. Zoller, Phys. Rev. A **94**, 033829 (2016).
[41] N. Somaschi, V. Giesz, L. De Santis, J. Loredo, M. P. Almeida, G. Hornecker, S. L. Portalupi, T. Grange, C. Antón, and J. Demory, Nat. Photon. **10**, 340 (2016).
[42] F. M. Faulstich, M. Kraft, and A. Carmele, J. Mod. Opt. **65**, 1323 (2018).
[43] S. J. Whalen, A. Grimsmo, and H. Carmichael, Quantum Sci. Technol. **2**, 044008 (2017).
[44] D. F. Walls and G. J. Milburn, *Quantum Optics* (Springer Science & Business Media, Berlin, 2007).
[45] J. C. Garrison and R. Y. Chiao, *Quantum Optics* (Oxford University Press, Oxford, 2008).
[46] N. L. Naumann, S. M. Hein, M. Kraft, A. Knorr, and A. Carmele, Proc. SPIE **10098**, 100980N (2017).
[47] See Supplemental Material at http://link.aps.org/supplemental/10.1103/PhysRevB.101.024305 for details in the derivation of the EOMs, steady-state formation, and stability analysis.
[48] K. Stannigel, P. Rabl, and P. Zoller, New J. Phys. **14**, 063014 (2012).
[49] L. C. Andreani, G. Panzarini, and J.-M. Gérard, Phys. Rev. B **60**, 13276 (1999).
[50] B. Krauskopf, in *Nonlinear Laser Dynamics: Concepts, Mathematics, Physics, and Applications International Spring School*, edited by B. Krauskopf and D. Lenstra, AIP Conf. Proc. No. 548 (AIP, Melville, NY, 2000), Vol. 548, pp. 1–30.
[51] R. Lang and K. Kobayashi, IEEE J. Quantum Electron. **16**, 347 (1980).
[52] R. W. Tkach and A. R. Chraplyvy, Electron. Lett. **21**, 1081 (1985).
[53] D. Lenstra, M. V. Vaalen, and B. Jaskorzyńska, Physica B+C **125**, 255 (1984).
[54] F. Albert, C. Hopfmann, S. Reitzenstein, C. Schneider, S. Höfling, L. Worschech, M. Kamp, W. Kinzel, A. Forchel, and I. Kanter, Nat. Commun. **2**, 366 (2011).
[55] T. Ramos, B. Vermersch, P. Hauke, H. Pichler, and P. Zoller, Phys. Rev. A **93**, 062104 (2016).
[56] H. Pichler, T. Ramos, A. J. Daley, and P. Zoller, Phys. Rev. A **91**, 042116 (2015).